Supplementary Information (SI) for Energy & Environmental Science.


# Isomeric Selenasumanene-Pyridine-Based Hole-Transporting Materials for Inverted Perovskite Solar Cells

Muhammad Azam[1†], Yao Ma[2†], Boxue Zhang[3†], Zhongquan Wan[1,*], Xiangfeng Shao[2,*], Haseeb Ashraf Malik[1], Xian Yang[5], Junsheng Luo[1,2,*] and Chunyang Jia[1,*]

[1] Dr. M. Azam, Dr. Z. Wan, Dr. H. A. Malik, Dr. J. Luo and Prof. C. Jia
National Key Laboratory of Electronic Films and Integrated Devices, School of Integrated Circuit Science and Engineering, University of Electronic Science and Technology of China, 611731 Chengdu, P. R. China
Email: cyjia@uestc.edu.cn

[2] Mr. Y. Ma, Prof. X. Shao
State Key Laboratory of Applied Organic Chemistry, Lanzhou University, Tianshui Southern Road 222, Lanzhou, 730000 Gansu Province, P. R. China
Email: shaoxf@lzu.edu.cn

[3] Mr. B. Zhang
Institut de Recherche de Chimie Paris (IRCP) UMR8247, Chimie ParisTech, PSL University CNRS, 11 rue P. et M. Curie, Paris F-75005, France

[4] Dr. J. Luo

Institute of Electronic and Information Engineering in Dongguan, University of Electronic Science and Technology of China, 523808 Dongguan, P. R. China

[5] Dr. X. Yang

School of Data Science, City University of Macau, Macau 999078, P. R. China

†These authors contributed equally to this work

## Experimental Section

### Materials

ITO glasses, lead iodide ($PbI_2$) and PCBM were purchased from Advanced Election Technology Co., Ltd. Ammonium salts Methylammonium bromide (MABr) and formamidinium iodide (FAI) were obtained from Greatcell Solar. Halogen salts including lead bromide ($PbBr_2$) and cesium iodide/bromide (CsI/Br) were purchased from Xi'an P-OLED. Perovskite solution process solvents, such as chlorobenzene (CB), isopropyl alcohol (IPA), dimethyl sulfoxide (DMSO) and N,N-dimethylformamide (DMF) were acquired from Sigma-Aldrich.

### Precursor solution preparation

For the HTL solution preparation, we have dissolved SePy-I/II powders in CB with different concentrations (2, 2.5, 3, 3.5 mg/mL) and put it in on the hotplate for stirring overnight to obtained desire solution. Triple cation perovskite precursor ($Cs_{0.05}FA_{0.85}MA_{0.10}PbI_3$) was prepared by dissolving CsI (19.5 mg) (0.0750 mmol), FAI (219.3 mg) (1.276 mmol), MAI (23.8mg) (0.1498 mmol), $PbI_2$ (760.7 mg) (1.650 mmol) (10% of excess) and MACl (12.5 Mol%) into DMF:DMSO = 4:1 vol. The corresponding solution was stirred for 2 h at room temperature. Electron transport precursor in CB was obtained by dissolving 20 mg/mL PCBM powder and stirred it overnight at 60 ˚C. Before using, all the solutions were filtered using 0.2 μm syringe filters.

### Device fabrication

Firstly, the ITO substrates (15 Ω square$^{-1}$) were consecutively washed with detergent, deionized water, acetone and ethanol, each washing step for 30 minutes duration under ultrasonic bath. Afterwards dry nitrogen stream was used to dry ITO glasses and put into $O_3$/ultraviolet surface treatment for 15 minutes. The hole transport layer was deposited using the stock solution of synthesised isomeric small molecules with the amount of 60 μL at 3000 rpm for 30 seconds, followed by annealing at 100 °C for 15 minutes in the glove box. After cool down to room temperature, the perovskite films were fabricated by spin-coating stock solution with volume of 70 μL onto the ITO/HTL substrates. The corresponding spin-coating was carried out in two steps, first at 1000 rpm for 10 seconds, and second at 5000 rpm for 45 seconds, respectively. During the second step, antisolvent CB with the volume of 200 μL was poured at the middle of the spinning substrate 10 s before the end of second step. Subsequently, the corresponding perovskite films were transferred to the hot plate for heating at 100 °C for 30 minutes.

**Deposition of ETL and Ag electrode**

The ETL was spin-coated on the perovskite substrates using PCBM stock solution at 3000 rpm for 30 seconds. BCP solution (0.5 mg/ml in isopropanol) was spin-coated on top of PCBM at 5000 rpm for 30 s, annealed 80 °C for 5 min. Finally, Ag metal back contact with thickness of 70 nm was thermally evaporated by a shadow mask at a pressure <$10^{-4}$ Pa.

**Photovoltaic measurements**

For the photovoltaic performance of PSCs, the JV characteristics measurements were performed on Keithley 2400 sourcemeter, with a standard solar simulator (Sirius-SS150A-D, Zolix Instruments Co. Ltd., Beijing, China). The illumination intensity was accurately calibrated to 100 $mWcm^{-2}$, confirming authenticity and alignment of the obtained results (calibrated using a standard silicon solar cell) under the ambient conditions. For the forward scan and revers scan, we have applied voltage ranges from -0.1 to 1.2 V and 1.2 to -0.1 V, respectively, using scanning rate of 0.01 mV $s^{-1}$. The active area of the prepared devices was evaluated to be 0.0812 $cm^2$ by an aperture mask.

**Characterization**

The structural analysis, XRD was performed on Panalytical X' Pert PRO with Cu Kα radiation. The redox potentials were obtained by CV on RST 5000 electrochemical analyzer with glassy carbon discs as the working electrode, Pt wire as the counter electrode, and SCE electrode as the reference electrode. Measurement conditions: solvent, $CH_2Cl_2$; concentration, $1\times10^{-4}$ mol $L^{-1}$; supporting electrolyte, $(n\text{-}Bu)_4NPF_6$ (0.1 M); scan speed, 50 mV $S^{-1}$; temperature, 20℃. The HOMO energy levels for SePy-I and SePy-II HTMs were estimated by employing following relation ($E_{HOMO} = -e\,(E_{ox}^{1} + 4.40)$), where the oxidation peak potentials for SePy-I and SePy-II were obtained from CV measurements (Figure 1i) and 4.40 is the absolute energy of reference electrode SCE vs. vacuum. To measure the wettability of novel HTMs we carried out water-contact angles measurements using drop shape analyzer

(Krüss DSA100). For getting the surface and cross-sectional morphologies of perovskite films based on different HTMs, we have employed SEM model (JEOL JSM-7600F). The PL results were obtained from HITACHI (model F-4600) spectrophotometer with the excitation wavelength of 485 nm. The TRPL analysis were performed by time correlated single photon counting (TCSPC) methodology with the same excitation wavelength with FluoroLog-3 Modular spectrofluorometer (HORIBA Jobin Yvon), the average lifetimes were calculated using TRPL measurements of three samples (ITO/perovskite, ITO/SePy-I/perovskite and ITO/SePy-II/perovskite) by a bi-exponential function: $Y = A_1 e^{(-\frac{t}{\tau_1})} + A_2 e^{(-\frac{t}{\tau_2})}$ and $< \tau > = \frac{A_1\tau_1^2 + A_2\tau_2^2}{A_1\tau_1 + A_2\tau_1}$, where $\tau$ is the carrier recombination lifetime, $\tau_1$ and $\tau_2$ are the decay components of the trap-assisted and radiative recombination process respectively. The obtained the charge transfer resistance in the whole device electronic impedance spectroscopy (EIS) measurements were performed on electrochemical workstation (CHI 760E, Shanghai Chenhua) with bias voltage of 10 mV under dark conditions. The respective results were fitted via Z-View equivalent circuit model to get the desire values. Space charge limiting current model: $n = \frac{2\varepsilon_o\varepsilon_r V_{TFL}}{eL^2}$ ($\varepsilon_o$, $\varepsilon_r$, $V_{TFL}$, e and L are vacuum permittivity, the dielectric constant, trap filled limited voltage, elementary charge, and film thickness, respectively) was used to execute the trap density using single hole only devices based on different HTL (ITO/SePy-I/II/PSK/Spiro-OMeTAD/Au) and recorded Dark *J-V* curves via Keithley 2400. Steady-state power output of respective devices was

performed under one sun (AM1.5G) illumination in ambient conditions at maximum power point tracking under reveres J-V scan with time interval of 100 seconds. The stabilized device PCE was measured by the product of voltage bias and current density values. All calculations were carried out with the Gaussian 16 programs. Geometry optimizations were carried out using B3LYP/Def2-SVP method. Molecular orbital energies and electrostatic potential were calculated at B3LYP/Def2-SVP level of theory using optimized structures. During the structure optimization and frontier orbital calculation, the butyl groups on SePy-I/II were replaced by methyls to give the corresponding (Schemes S1 and S2), as they have almost no contribution on the HOMO and LUMO orbitals and the geometry of the conjugated framework.

**Stability measurements**

For the authentic stability test under moisture and thermal stresses, we have prepared the five devices based on SePy-I and SePy-II HTMs. For the long-term humidity-stability test, the un-encapsulated devices were aged in ambient environment with relative humidity (RH = 30-40%), and recorded the device performance after different time intervals. Similarly, to perform thermal stability test, the respective devices were aged at 85 °C under nitrogen environment. The operational stability test was performed on unencapsulated devices aged at 65 °C in $N_2$-filled chambers under metal halide lamps based on UV filters.

**Synthesis of SePy-I**

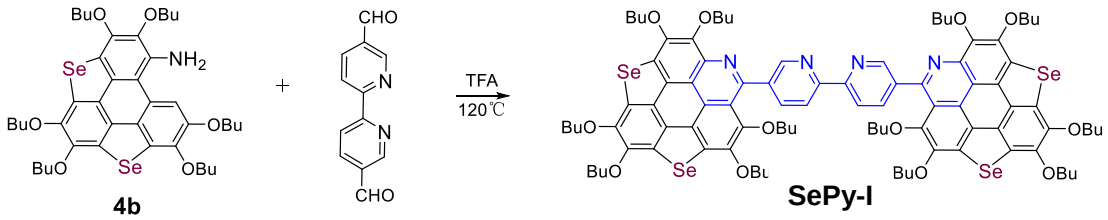


**Scheme S1:** Synthesis route of SePy-I.

The **4b** (0.41 g, 0.5 mmol) and 2,2'-Bipyridine-5,5'-dicarboxaldehyde (0.042g, 0.2 mmol) were dissolved in TFA (3 mL) and sealed in a Schlenk tube. The resulting mixture was heated with stirring at 120 ˚C for 12 h. After the reaction was finished, the reaction mixture was diluted with $CH_2Cl_2$ and neutralized with $NaHCO_3$, extracted with $CH_2Cl_2$ (3 × 10 mL). The organic layer was dried with anhydrous $Na_2SO_4$, then concentrated under reduced pressure. The crude product was recrystallized from EA/DCM (10 : 1, *v/v*) to give **SePy-I** as a yellow powder (0.22 g, 60% yield). For **SePy-I**, mp: 256.5-257.3 °C; $^1$H NMR (600 MHz, Chloroform-d) δ 9.27 (s, 2H), 8.66 (s, 2H), 8.54 (s, 2H), 4.77–4.50 (m, 20H), 3.85–3.57 (m, 4H), 2.12–1.89 (m, 20H), 1.85–1.61 (m, 20H), 1.23–1.02 (m, 38H), 0.80–0.67 (m, 6H); $^{13}$C NMR (151 MHz, $CDCl_3$) δ 155.6, 155.5, 151.5, 150.1, 149.8, 149.1(2), 148.2(2), 148.1, 147.1, 146.3, 135.7, 134.1, 134.0, 129.8, 129.8, 129.6(2), 128.8(2), 128.5, 127.0, 125.8(2), 125.3(2), 124.8, 123.2, 122.5, 116.9, 113.7, 75.9, 75.2, 73.6, 73.2, 73.1, 72.8, 32.6(2), 32.5(2), 32.4, 31.3, 19.4(3), 19.0, 14.0(2), 13.9, -0.00; IR (KBr) v 3435, 2957, 2932, 2871, 1534, 1464, 1411, 1357, 1117, 1095, 1063, 1020, 948, 845, 750; High resolution mass spectrometry (HRMS): calculated for ($C_{96}H_{114}N_4O_{12}Se_4$+H), 1834.5208; found, 1834.5247.

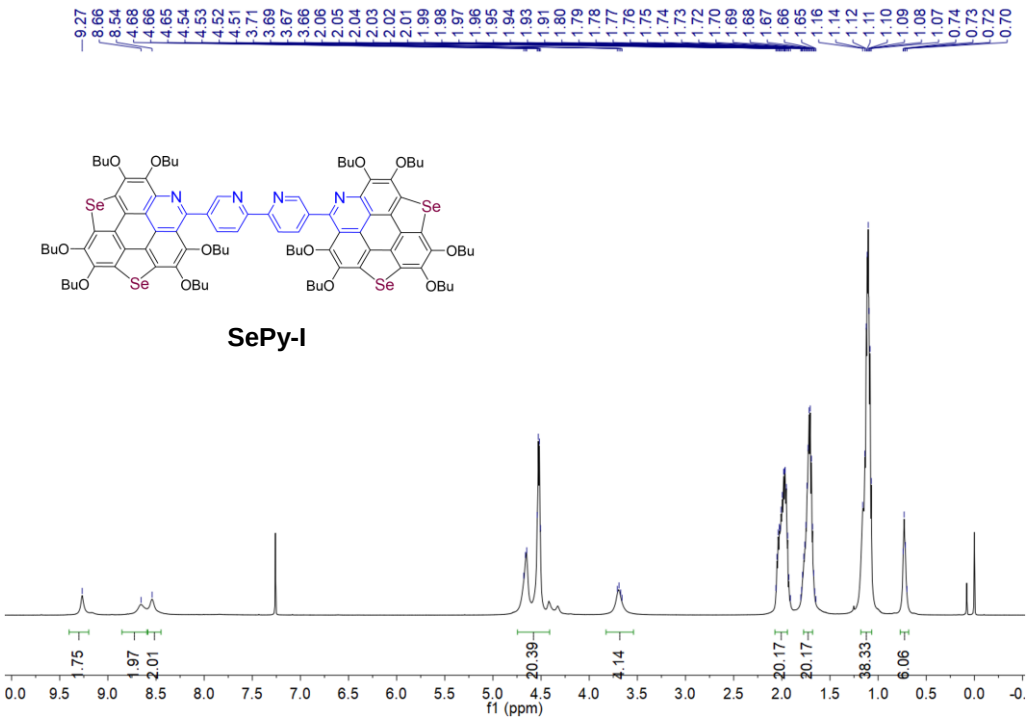


**Figure S1** $^{1}$H NMR spectrum of molecule SePy-I.

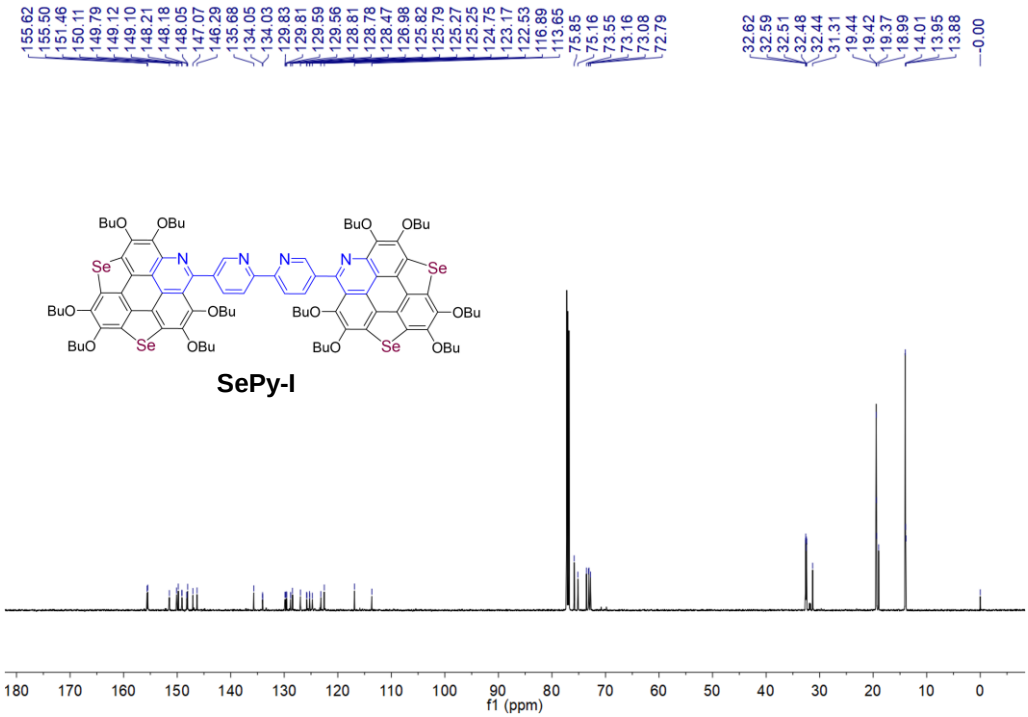


**Figure S2** $^{13}$C NMR spectrum of molecule SePy-I.

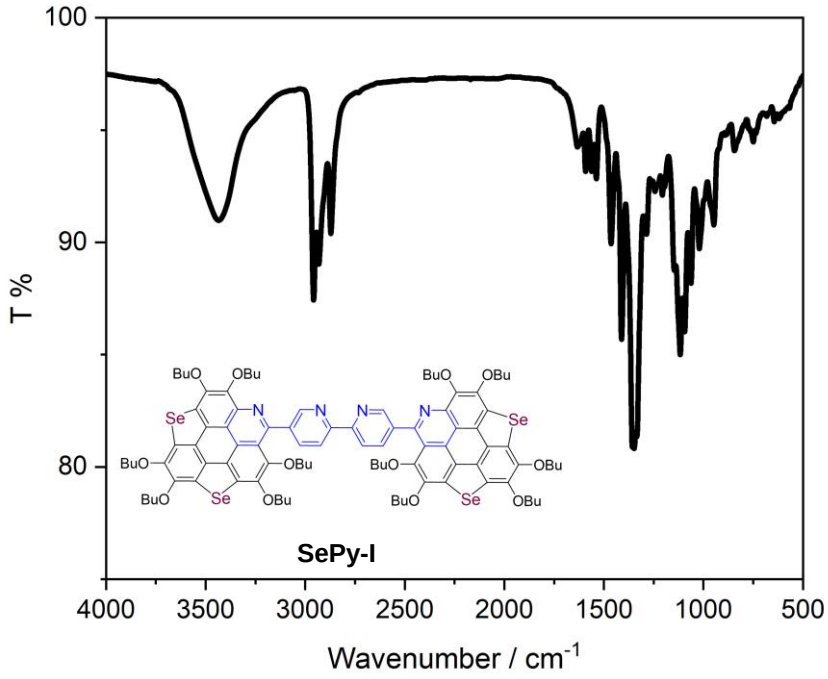


**Figure S3** FTIR spectrum of molecule SePy-I.

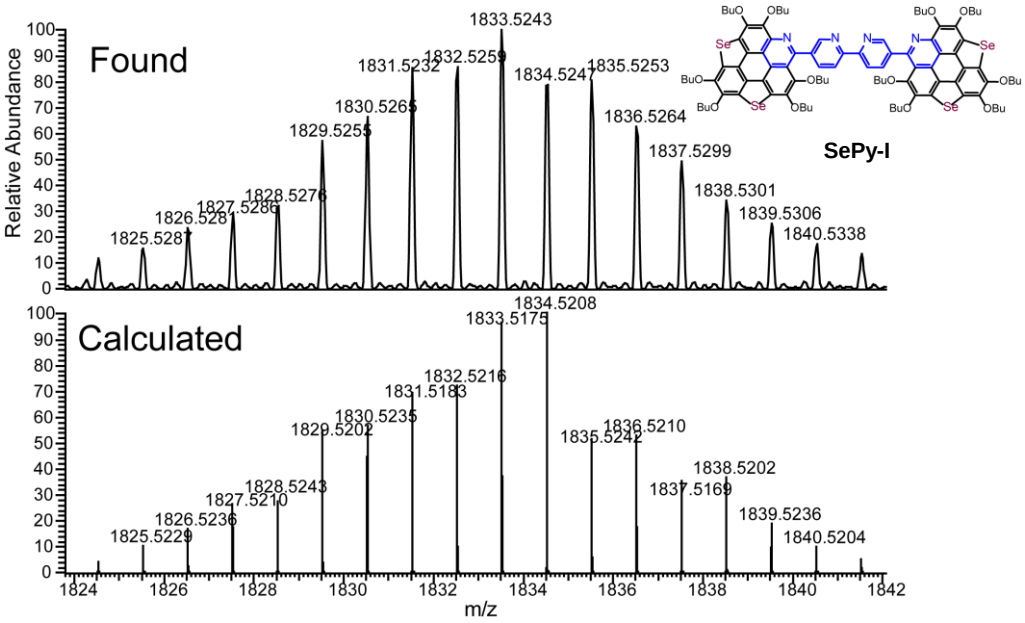


**Figure S4** HRMS spectra theoretical and experimental comparison of molecule SePy-I.

**Synthesis of SePy-I**

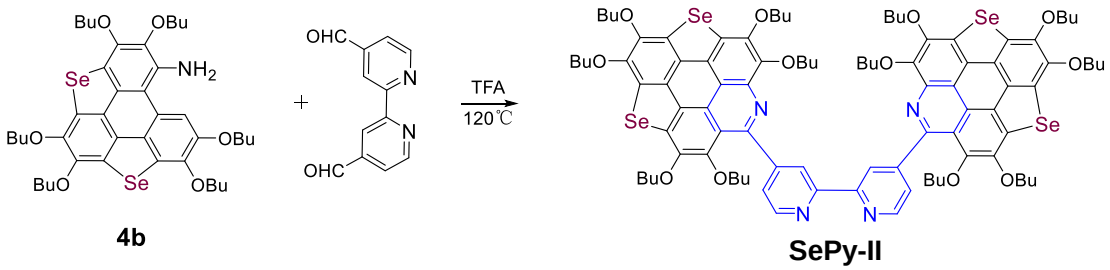


**Scheme S2.** Synthesis route of SePy-II.

The **4b** (0.41 g, 0.5 mmol) and 2,2'-Bipyridine-4,4'-dicarboxaldehyde (0.042 g, 0.2 mmol) were dissolved in TFA (3 mL) and sealed in a Schlenk tube. The resulting mixture was heated with stirring at 120 ˚C for 12 h. After the reaction was finished, the reaction mixture was diluted with $CH_2Cl_2$ and neutralized with $NaHCO_3$, extracted with $CH_2Cl_2$ (3 × 10 mL). The organic layer was dried with anhydrous $Na_2SO_4$, then concentrated under reduced pressure. The crude product was recrystallized from EA/DCM (10 : 1, *v/v*) to give **SePy-II** as a yellow powder (0.20 g, 55% yield). For **SePy-II**, mp: 214.5-215.3 °C; $^1$H NMR (600 MHz, Chloroform-d) δ 9.07 (s, 2H), 8.85 (d, J = 4.9 Hz, 2H), 7.85 (d, J = 4.8 Hz, 2H), 4.69 (t, J = 6.6 Hz, 4H), 4.62–4.48 (m, 16H), 3.79 (t, J = 6.4 Hz, 4H), 2.01–1.93 (m, 16H), 1.91–1.85 (m, 4H), 1.75–1.65 (m, 16H), 1.65–1.59 (m, 4H), 1.18–1.12 (m, 8H), 1.12–0.97 (m, 30H), 0.75 (t, J = 6.9 Hz, 6H); $^{13}$C NMR (151 MHz, $CDCl_3$) δ 155.6, 155.5, 151.5, 150.1, 149.8, 149.2, 148.2, 148.1, 147.1, 146.3, 135.7, 134.1, 129.9, 129.6, 128.8, 128.5, 127.0, 125.9, 125.3, 124.7, 123.2, 122.6, 116.9, 113.7, 75.9, 75.2, 73.6, 73.2, 73.1, 72.8, 32.6(2), 32.5(2), 32.4, 31.3, 19.4(3), 19.0, 14.00(2), 13.9; IR (KBr) v 3424, 2958, 2932, 2871,

1591, 1540, 1462, 1411, 1357, 1333, 1117, 1094, 1062, 946, 843 $cm^{-1}$. HRMS: calculated for ($C_{96}H_{114}N_4O_{12}Se_4$+H), 1834.5208; found, 1834.5234.

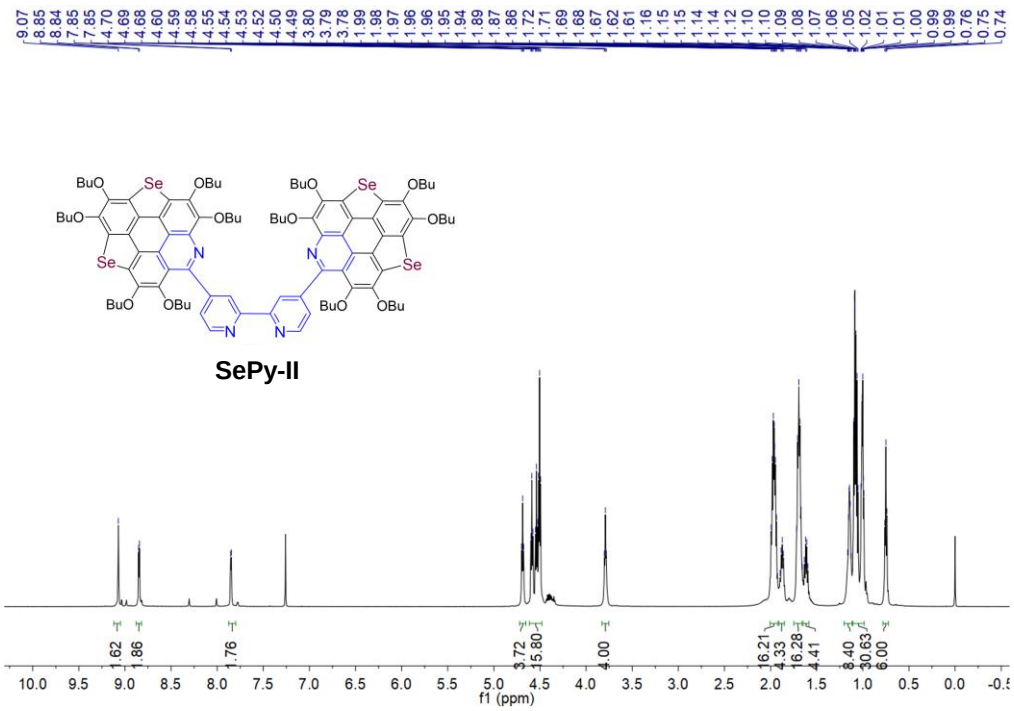


**Figure S5** $^{1}$H NMR spectrum of molecule SePy-II.

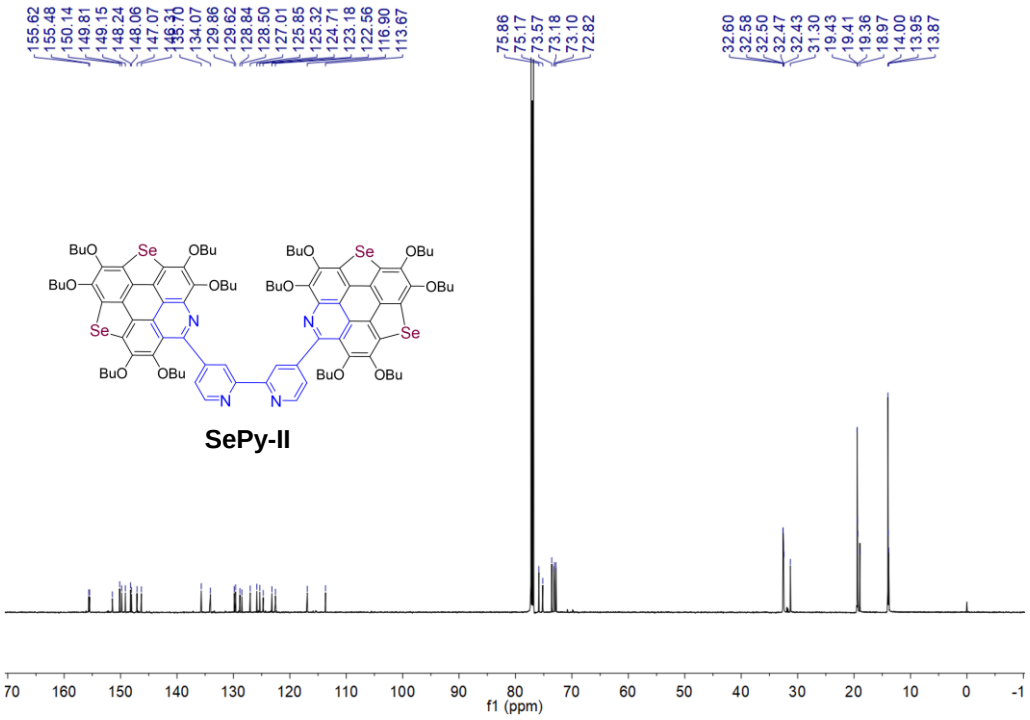


**Figure S6** $^{13}$C NMR spectrum of molecule SePy-II.

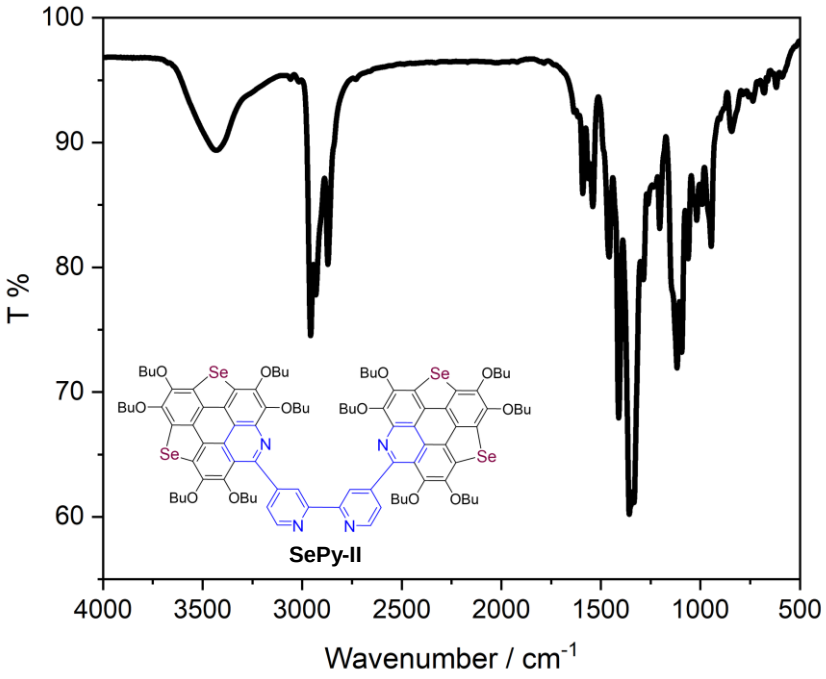


**Figure S7** FTIR spectrum of molecule SePy-II.

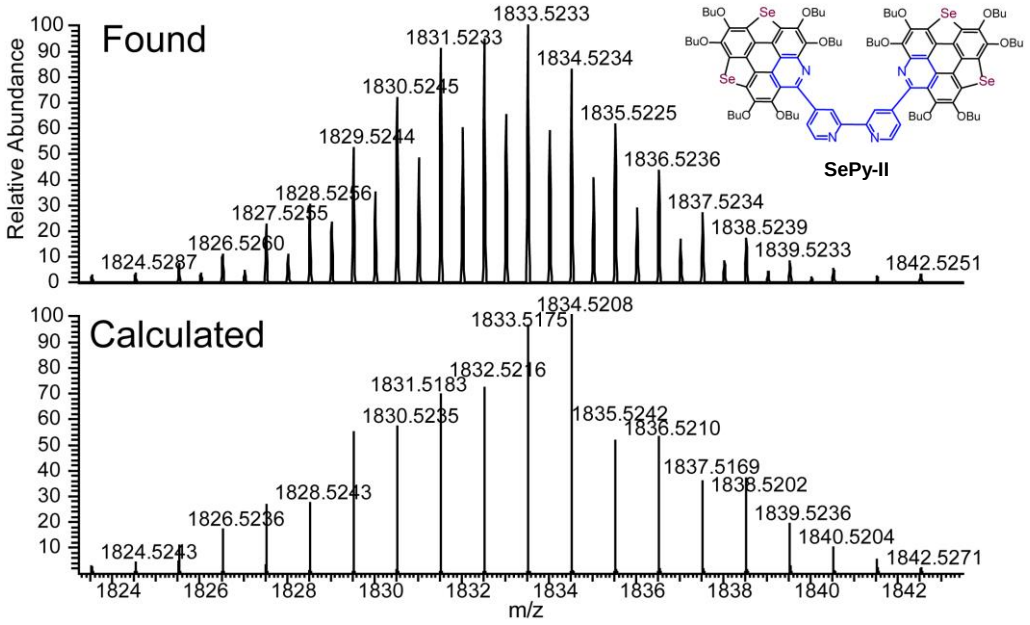


**Figure S8** HRMS spectra theoretical and experimental comparison of molecule SePy-II.

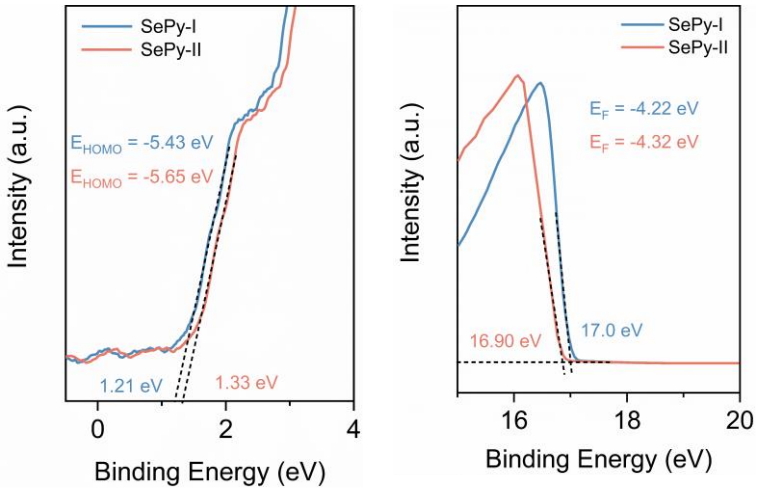


**Figure S9** Onset and cut-off regions of the UPS spectra for SePy-I and SePy-II.

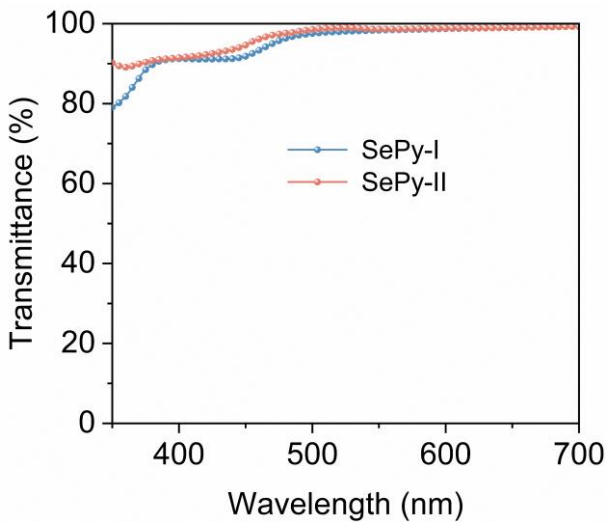


**Figure S10** Transmittance analysis of films SePy-I and SePy-II.

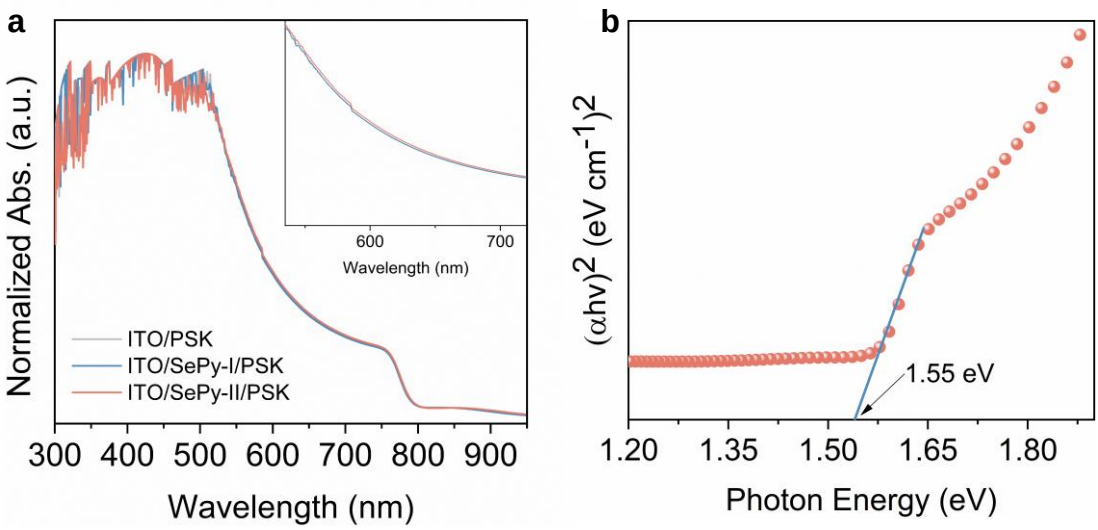


**Figure S11** Absorption spectra of perovskite films spin-coated on different HTLs.

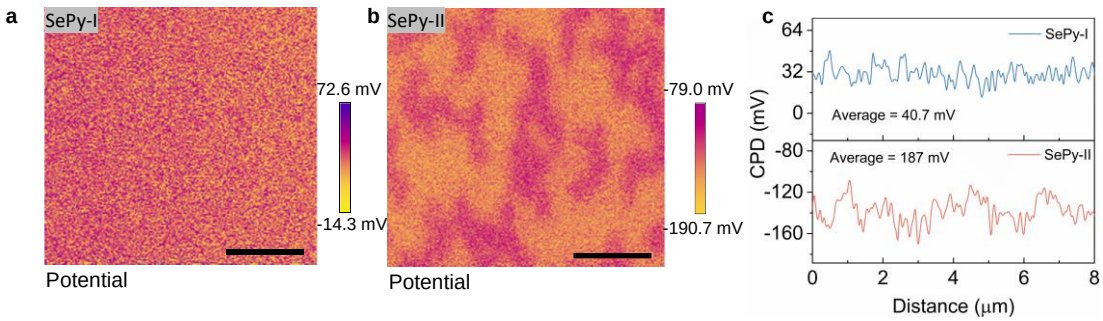


**Figure S12** KPFM images of SePy-I (a) and SePy-II (b) films. c) CPD measurement of corresponding HTLs.

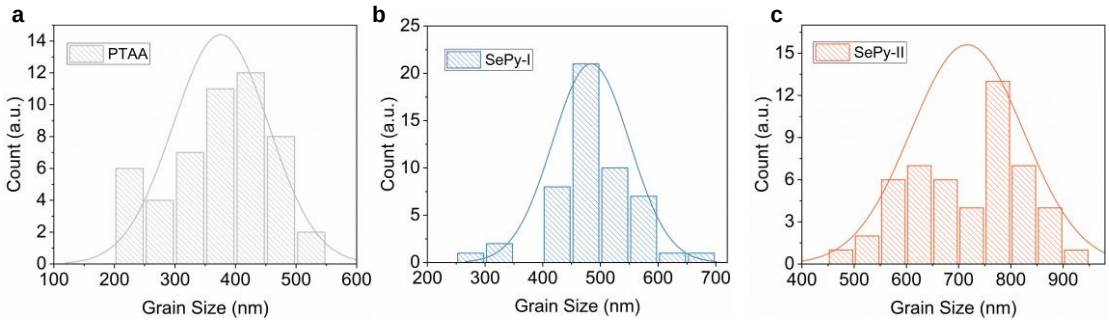


**Figure S13** Statistical grain-size distribution of perovskite films based on different HTMs.

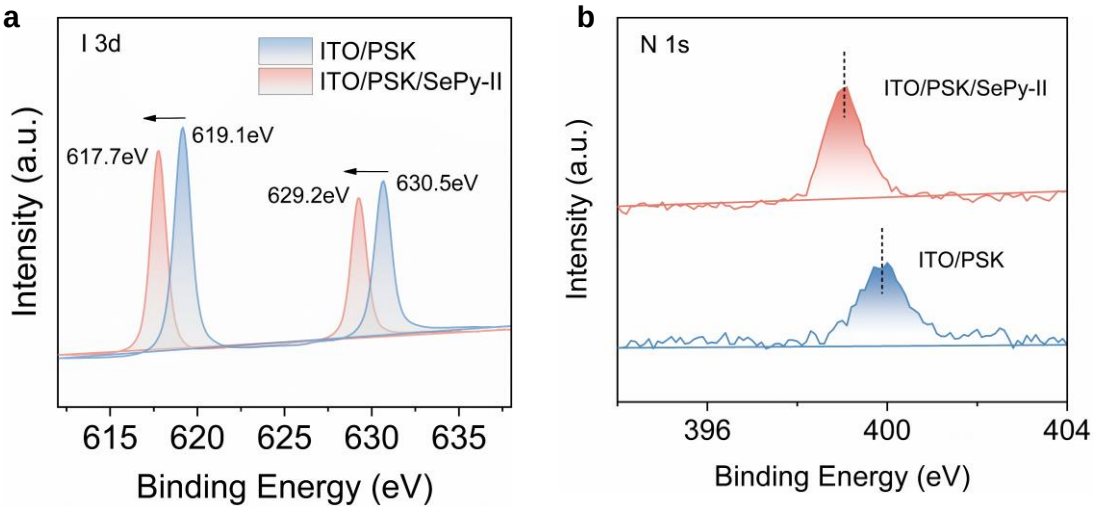


**Figure S14** High-resolution I 3d (a) and N 1s (b) XPS spectra of the perovskite films without and with SePy-II capping.

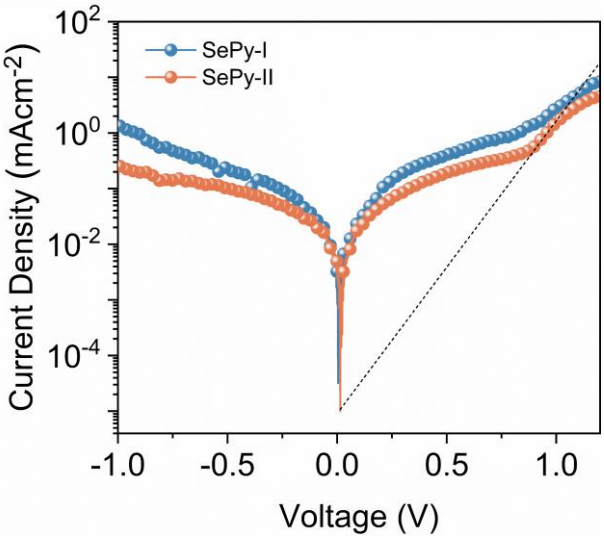


**Figure S15** Dark J-V curves of PSCs based on SePy-I and SePy-II HTMs.

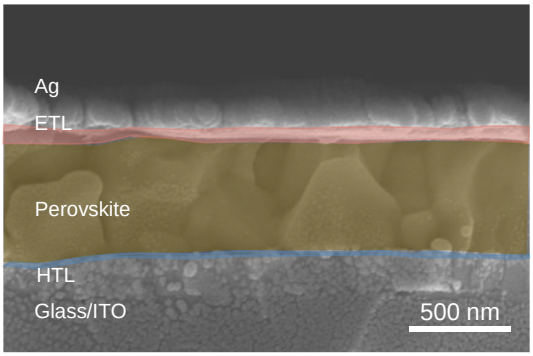


**Figure S16** Cross-sectional SEM image of corresponding fabricated p-i-n device.

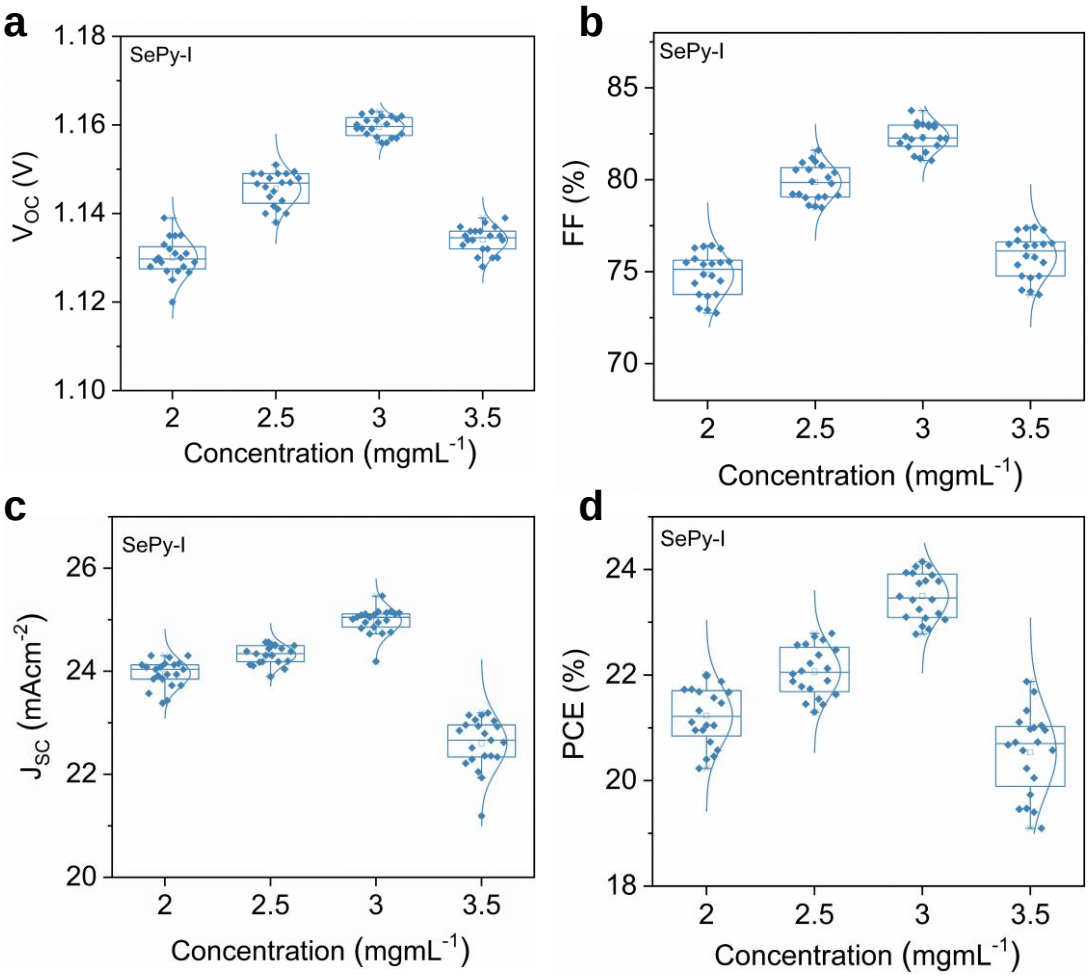


**Figure S17** Photovoltaic parameters with different concentration of SePy-I.

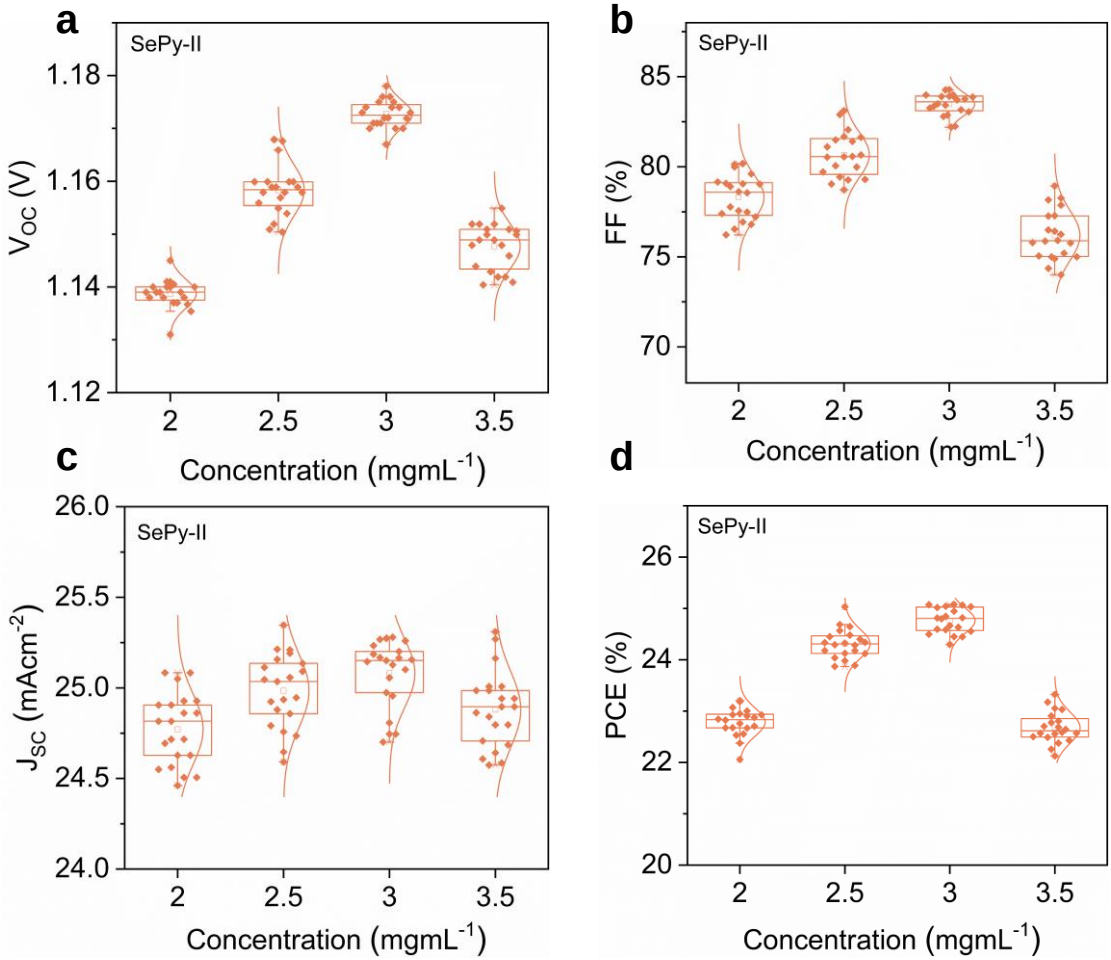


**Figure S18** Photovoltaic parameters with different concentration of SePy-II.

220021349274

# Test Report

Test Report No. AGXB124W00584

| | |
|---|---|
| Subject unit | Perovskite solar cells |
| Manufacturer | University of Electronic Science and Technology of China |
| Commission unit | University of Electronic Science and Technology of China |
| Inspection category | Commissioned inspection |

Chengdu Institute of Product Quality Inspection Co., Ltd.

National Photovoltaic Product Quality Inspection & Testing Center

# Chengdu Institute of Product Quality Inspection Co., Ltd.
## National Photovoltaic Product Quality Inspection &Testing Center
## TEST REPORT

Test Report No.AGXB124W00584 

| | | | |
|---|---|---|---|
| Product Name | Perovskite solar cells | Trade Mark | / |
| Manufacture Date | / | Model /Type | 2.5cm×2.5cm |
| Sample No. | AGXB124W00584 | Sample Grade | / |
| Sample Quantity | One piece | Sample State | / |
| Delivery Date | 21/10/2024 | Sample Delivered personnel | Muhammad Azam |
| Commission unit | University of Electronic Science and Technology of China | Manufacturer | University of Electronic Science and Technology of China |
| Commission unit addres | No.2006, Xiyuan Ave, West Hi-Tech Zone, Chengdu, P. R. China | Manufacturer Address | No.2006, Xiyuan Ave, West Hi-Tech Zone, Chengdu, P. R. China |
| Commission unit Zip code | 611731 | Manufacturer Zip code | 611731 |
| Commission unit Tel. | 18582510740 | Manufacturer Tel. | 18582510740 |
| Center Address | No. 355, 2nd Tengfei Road, Southwest Airport Economic Development Zone, Chengdu, Sichuan, P. R. China. | Measurement Date | 21/10/2024 |
| Methods | IEC 60904-1:2020 Photovoltaic devices-Part 1: Measurement of Photovoltaic Current-Voltage Characteristics. | | |
| Test conclusion | This column blank. | | |
| Remarks | (Special Chapter for test report)<br>Issue Date: 24/10/2024<br>The mask area is provided by the Commission unit: 0.0812cm². | | |

**Approved by** 钱鹏楠 **Reviewed by** 许雅 **Measured by** 游宗英

**Test Results（Forward scanning）:**

| No. | Test item(s) | Unit | Results |
|---|---|---|---|
| 1 | Current-voltage characteristics measurement | --- | --- |
| 1.1 | Open-circuit voltage, $V_{OC}$ | V | 1.161 |
| 1.2 | Short-circuit current, $I_{SC}$ | mA | 2.057 |
| 1.3 | Maximum-power, $P_{max}$ | mW | 1.981 |
| 1.4 | Maximum-power voltage, $V_{p\text{-}max}$ | V | 1.020 |
| 1.5 | Maximum-power current, $I_{p\text{-}max}$ | mA | 1.942 |
| 1.6 | Fill factor, FF | % | 82.94 |
| 1.7 | Conversion efficiency, η | % | 24.40 |

Current-voltage characteristics

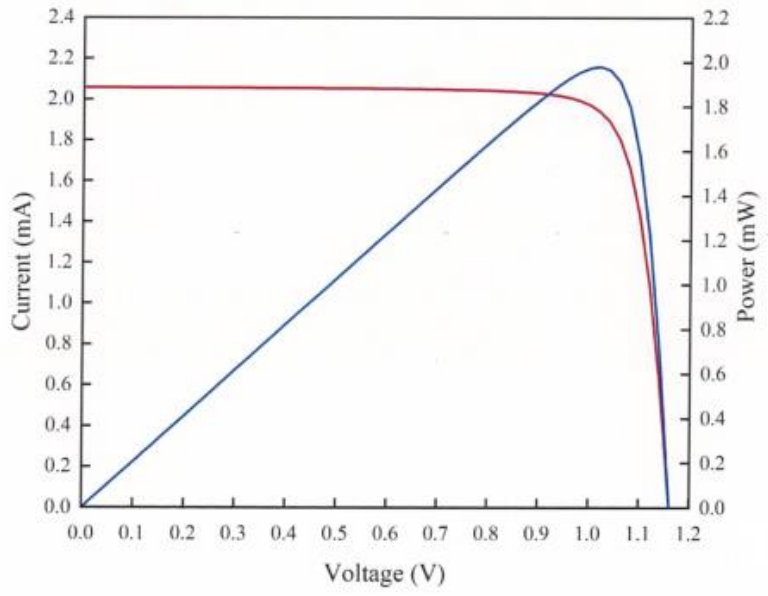


**Remark:** Sample was tested under the irradiation with a steady-state class calibrated AAA solar simulator (AM1.5-G 1000.0 W/m² basted on mono-Si reference cell) at 25±1 °C. Designated area defined by thin metal aperture mask.
The measuring uncertainty : $U_{rel}$(Pmax)=2.85%(k=2); $U_{rel}$(Isc)=2.69%(k=2); $U_{rel}$(Voc)=1.57%(k=2).

Chengdu Institute of Product Quality Inspection Co., Ltd.
National Photovoltaic Product Quality Inspection &Testing Center
TEST REPORT

Test Report No. AGXB124W00584 Page 3 of 3

**Test Results（Reverse scanning）:**

| No. | Test item(s) | Unit | Results |
|---|---|---|---|
| 2 | Current-voltage characteristics measurement | --- | --- |
| 2.1 | Open-circuit voltage, $V_{OC}$ | V | 1.164 |
| 2.2 | Short-circuit current, $I_{SC}$ | mA | 2.056 |
| 2.3 | Maximum-power, $P_{max}$ | mW | 2.006 |
| 2.4 | Maximum-power voltage, $V_{p\text{-}max}$ | V | 1.020 |
| 2.5 | Maximum-power current, $I_{p\text{-}max}$ | mA | 1.967 |
| 2.6 | Fill factor, FF | % | 83.84 |
| 2.7 | Conversion efficiency, η | % | 24.70 |

Current-voltage characteristics under STC

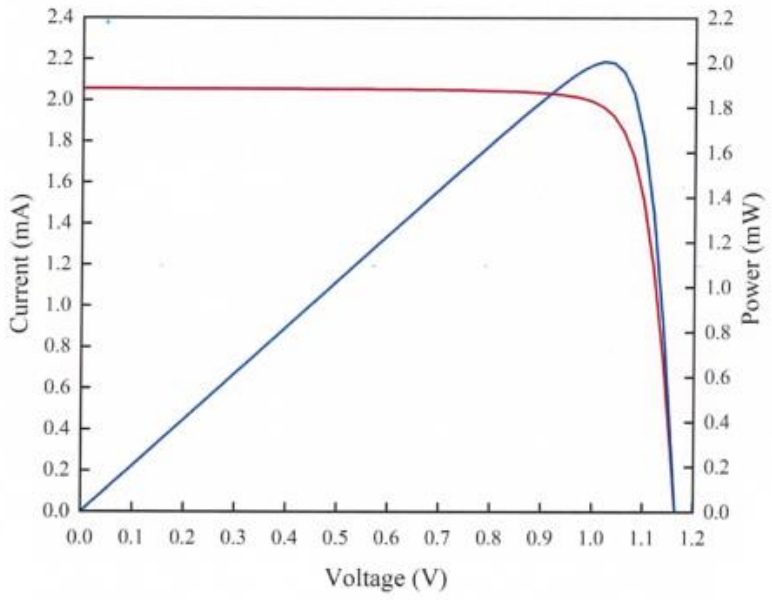


**Remark:** Sample was tested under the irradiation with a steady-state class calibrated AAA solar simulator (AM1.5-G 1000.0 W/m² basted on mono-Si reference cell) at 25±1 ℃. Designated area defined by thin metal aperture mask.
The measuring uncertainty : $U_{rel}$(Pmax)=2.85%(k=2); $U_{rel}$(Isc)=2.69%(k=2); $U_{rel}$(Voc)=1.57%(k=2).

Blank

**Figure S19** Certification of record PCE of our champion device based on SePy-II based HTM.

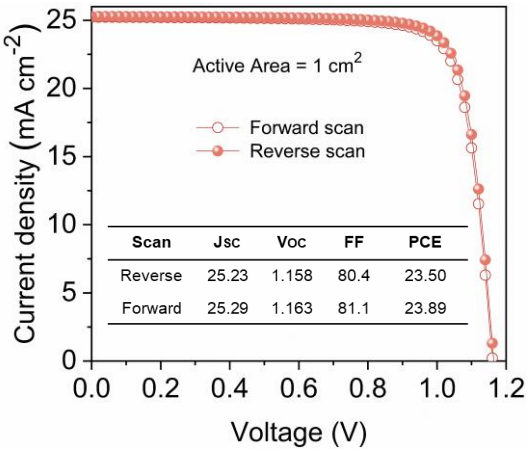


**Figure S20** J-V curves of device based on SePy-II HTM with an active area of 1 $cm^2$ (inset given the device parameters under reverse and forward scan).

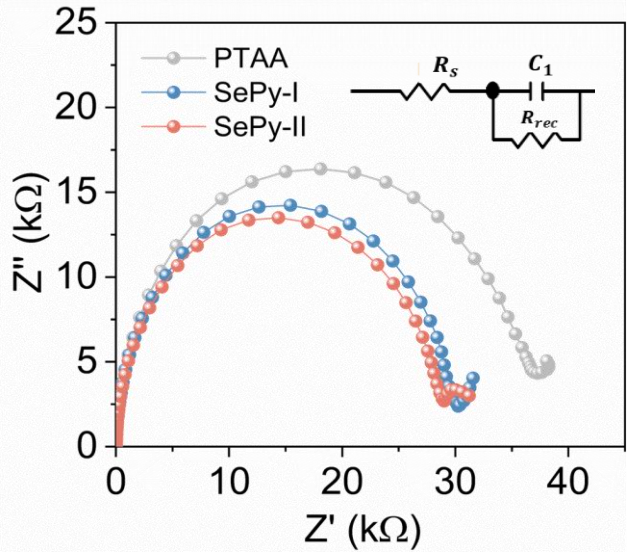


**Figure S21** Nyquist plots of corresponding devices with inset shows equivalent circuit diagram for fitting.

**Table S1**: The average decay lifetime of charge carriers with different decay components obtained from fitting of PL decay curves with a bi-exponential function.

| **Sample** | **$A_1$** | **$\tau_1$ (ns)** | **$A_2$** | **$\tau_2$ (ns)** | **$\langle\tau\rangle$ (ns)** |
|---|---|---|---|---|---|
| ITO/PSK | 2545.71 | 60.232 | 5228.67 | 177.35 | 160.732 |
| ITO/SePy-I/PSK | 2250.23 | 46.67 | 8237.86 | 97.45 | 91.5755 |
| ITO/SePy-II/PSK | 1627.89 | 48.4 | 6305.67 | 51.7 | 51.0577 |

**Table S2.** Summary of PCEs and stability of inverted PSCs based on various small molecules HTMs.

| HTMs | Device Structure | PCE (%) | Aging Conditions | PCE Loss | Ref |
|---|---|---|---|---|---|
| DFTAB | ITO/DFTAB/perovskite/PCBM/Ag | 12.4 | Encapsulation: No<br>Light intensity: No<br>Temperature: No<br>Duration: No | N/A | [1] |
| TAE | ITO/TAE/perovskite/PCBM/Ag | 11.5 | Encapsulation: No<br>Light intensity: No<br>Temperature: No<br>Duration: No | N/A | [1] |
| Trux-OMeTAD | ITO/Trux-OMeTAD/perovskite/PCBM/ZnO NP/Al | 18.6 | Encapsulation: No<br>Light intensity: No<br>Temperature: No<br>Duration: No | N/A | [2] |
| TPAC0M | ITO/TPAC0M/perovskite/PCBM/ ZnO NP/Al | 13.92 | Encapsulation: No<br>Light intensity: No<br>Temperature: No<br>Duration: No | N/A | [3] |
| TPAC2M | ITO/TPAC2M/perovskite/PCBM/ ZnO NP/Al | 15.77 | Encapsulation: No<br>Light intensity: No<br>Temperature: No<br>Duration: No | N/A | [3] |
| TPAC3M | ITO/TPAC3M/perovskite/PCBM/ ZnO NP/Al | 17.54 | Encapsulation: No<br>Light intensity: No<br>Temperature: No<br>Duration: No | N/A | [3] |
| TP-FTzF-TP | ITO/TP-FTzF- | 16.4 | Encapsulation: No | N/A | [4] |

| | | | | | |
|---|---|---|---|---|---|
| | TP/perovskite/PCBM/Au | | Light intensity: No<br>Temperature: No<br>Duration: No | | |
| m-MTDATA | ITO/m-MTDATA/perovskite/$C_{60}$/BCP/Cu | 18.12 | Encapsulation: No<br>Light intensity: No<br>Temperature: No<br>Duration: 1000 h in ambient | 10% | [5] |
| H1 | ITO/H1/perovskite/PCBM/LiF/Al | 13.5 | Encapsulation: No<br>Light intensity: No<br>Temperature: No<br>Duration: No | N/A | [6] |
| H2 | ITO/H2/perovskite/PCBM/LiF/Al | 13.3 | Encapsulation: No<br>Light intensity: No<br>Temperature: No<br>Duration: No | N/A | [6] |
| TPA-2,7-FLTPA-TPA & TPA-3,6-FLTPA-TPA | ITO/$MoO_3$/HTL/perovskite/$C_{60}$/BCP/Ag | 17.1 | Encapsulation: No<br>Light intensity: No<br>Temperature: No<br>Duration: No | N/A | [7] |
| FB-OMeTPA & FT-OMeTPA | ITO/HTL/perovskite/PCBM/BCP/Ag | 17.57 | Encapsulation: No<br>Light intensity: No<br>Temperature: No<br>Duration: No | N/A | [8] |
| BT, QT and HT | ITO/HTL/perovskite/PCBM/BCP/Ag | 17.69 | Encapsulation: No<br>Light intensity: No<br>Temperature: No<br>Duration: No | N/A | [9] |
| XY1 | ITO/XY1/perovskite/$C_{60}$/BCP/Cu | 18.78 | Encapsulation: No | 14% | [10] |

| | | | | | |
|---|---|---|---|---|---|
| | | | Light intensity: 100 $mWcm^{-2}$ Temperature: No Duration:480 h in $N_2$ | | |
| $C_8$-DPNDF | ITO/$C_8$-DPNDF/perovskite/$C_{60}$/BCP/Ag | 17.5 | Encapsulation: No Light intensity: No Temperature: No Duration:30 h in ambient RH=40% | 8% | [11] |
| H2 | ITO/H2/perovskite/PCBM/BCP/Ag | 18.69 | Encapsulation: No Light intensity: No Temperature: RT Duration: 200 h in ambient RH=60% | N/A | [12] |
| D−A−D organic | ITO/$NiO_x$/organic HTM/perovskite/PCBM/BCP/Ag | 20.22 | Encapsulation: No Light intensity: No Temperature: RT Duration: 500 h in $N_2$ | 5% | [13] |
| DBTMT | ITO/DBTMT/perovskite/$C_{60}$/BCP/Ag | 21.12 | Encapsulation: No Light intensity: No Temperature: RT Duration:60 h in ambient RH=60-80% | 34% | [14] |
| TPE-S | ITO/TPE-S/$FA_{0.9}Cs_{0.1}PbI_3$/PCBM/ZnO/Ag | 21.0 | Encapsulation: No Light intensity: No Temperature: No Duration: No | N/A | [15] |
| MPA-Cz-BTI | ITO/MPA-Cz-BTI/perovskite/$C_{60}$/BCP/Ag | 21.35 | Encapsulation: Yes Light intensity: 100 | 20% | [16] |

| | | | | | |
|---|---|---|---|---|---|
| | | | mWcm$^{-2}$<br>Temperature: RT<br>Duration:900 h in ambient RH=60% | | |
| H-Pyr | ITO/H-Pyr/perovskite/PCBM/Ag | 17.09 | Encapsulation: No<br>Light intensity: No<br>Temperature: RT<br>Duration:500 h in RH of 55% | 20% | [17] |
| D2 | ITO/D2/perovskite/PCBM/BCP/Ag | 17.45 | Encapsulation: No<br>Light intensity: No<br>Temperature: RT<br>Duration: 1440 h in ambient | 20% | [18] |
| DPh-DNTT | ITO/MeO-2PACz/3FPIP/perovskite/Spiro-OMeTAD/$MoO_x$/Ag | 20.2 | Encapsulation: No<br>Light intensity: No<br>Temperature: RT<br>Duration: 1080 h in ambient RH=60% | 10% | [19] |
| BTF5 & BTF6 | ITO/BTF5/perovskite/$C_{60}$/BCP/Ag | 20.34 | Encapsulation: No<br>Light intensity: 100 mWcm$^{-2}$<br>Temperature: RT<br>Duration:500 h in $N_2$ | 0% | [20] |
| DTT | ITO/DTT/perovskite/$C_{60}$/BCP/Ag | 19.23 | Encapsulation: No<br>Light intensity: No<br>Temperature: RT<br>Duration: 150 h in ambient RH=50% | 45% | [21] |

| | | | | | |
|---|---|---|---|---|---|
| DMeTPA-O | ITO/DMeTPA-O/perovskite/$C_{60}$/BCP/Ag | 20.57 | Encapsulation: No<br>Light intensity: No<br>Temperature: No<br>Duration: No | N/A | [22] |
| DFBT-PMTP | ITO/DFBT-PMTP/perovskite/$C_{60}$/BCP/Ag | 21.23 | Encapsulation: No<br>Light intensity: No<br>Temperature: 65 ˚C<br>Duration: 145 h in ambient RH=40% | 20% | [23] |
| CL-MCz | ITO/CL-MCz/perovskite/$C_{60}$/BCP/Ag | 23.9 | Encapsulation: No<br>Light intensity: 100 $mWcm^{-2}$<br>Temperature: RT<br>Duration: 500 h in $N_2$ | 9% | [24] |
| TPASF & TPAOF | ITO/TPASF/perovskite/$C_{60}$/BCP/Ag | 21.01 | Encapsulation: No<br>Light intensity: 100 $mWcm^{-2}$<br>Temperature: 35 ˚C<br>Duration: 632 h in $N_2$ | 20% | [25] |
| TPA-CAA | FTO/TPA-CAA/perovskite/$C_{60}$/BCP/Ag | 21.56 | Encapsulation: No<br>Light intensity: No<br>Temperature: RT<br>Duration: 1000 h in ambient RH=30-40% | 20% | [26] |
| BTP1-2 | ITO/BTP1-2/perovskite/$C_{60}$/BCP/Ag | 24.34 | Encapsulation: No<br>Light intensity: 100 $mWcm^{-2}$<br>Temperature: 35 °C<br>Duration: 528 h in $N_2$ | 15% | [27] |

| | | | | | |
|---|---|---|---|---|---|
| C3-D | ITO/C3-S/perovskite/$PC_{61}BM$/BCP/Ag | 21.50 | Encapsulation: No<br>Light intensity: 100 $mWcm^{-2}$<br>Temperature: RT<br>Duration: 500 h in ambient RH=35-40% | 15% | [28] |
| A1090B769 | ITO/A1090B769/perovskite/PCBM/BCP/Ag | 26.2 | Encapsulation: No<br>Light intensity: 100 $mWcm^{-2}$<br>Temperature: 65 °C<br>Duration: 1000 h in $N_2$ | 20% | [29] |
| SFT-STPA | ITO/SFT-STPA/perovskite/$C_{60}$/BCP/Cu | 26.1 | Encapsulation: No<br>Light intensity: 100 $mWcm^{-2}$<br>Temperature: 65 °C<br>Duration: 1000 h in $N_2$ | 6 | [30] |
| SePy-II | ITO/SePy-II/perovskite/$PC_{61}BM$/BCP/Ag | 25.05 | Encapsulation: No<br>Light intensity: 100 $mWcm^{-2}$<br>Temperature: 65 °C<br>Duration: 1230 h in $N_2$ | 6% | This Work |

## References


[1] A. E. Labban, H. Chen, M. Kirkus, J. Barbe, S. Del Gobbo, M. Neophytou, I. McCulloch, J. Eid, *Adv. Energy Mater.* **2016**, 6, 1502101.

[2] C. Huang, W. Fu, C.-Z. Li, Z. Zhang, W. Qiu, M. Shi, P. Heremans, A. K. Y. Jen, H. Chen, *J. Am. Chem. Soc.* **2016**, 138, 2528.

[3] S. J. Park, S. Jeon, I. K. Lee, J. Zhang, H. Jeong, J.-Y. Park, J. Bang, T.

K. Ahn, H.-W. Shin, B.-G. Kim, H. J. Park, *J. Mater. Chem. A* **2017**, 5, 13220.

[4] S. Ameen, M. S. Akhtar, M. Nazim, M. K. Nazeeruddin, H.-S. Shin, *Nano Energy* **2018**, 49, 372.

[5] R. Chen, T. Bu, J. Li, W. Li, P. Zhou, X. Liu, Z. Ku, J. Zhong, Y. Peng, F. Huang, Y.-B. Cheng, Z. Fu, *ChemSusChem* **2018**, 11, 1467.

[6] R. Iacobellis, S. Masi, A. Rizzo, R. Grisorio, M. Ambrico, S. Colella, P. F. Ambrico, G. P. Suranna, A. Listorti, L. De Marco, *ACS Appl. Energy Mater.* **2018**, 1, 1069.

[7] H. D. Pham, L. Gil-Escrig, K. Feron, S. Manzhos, S. Albrecht, H. J. Bolink, P. Sonar, *J. Mater. Chem. A* **2019**, 7, 12507.

[8] F. Meng, Y. Jia, J. Wang, X. Huang, Z. Gui, L. Huang, R. Li, R. Chen, J. Xu, W. Chen, Z. He, H.-Y. Hsu, E. Zhu, G. Che, H.-L. Wang, *Sol. RRL* **2019**, 3, 1900319.

[9] E. Li, W. Li, L. Li, H. Zhang, C. Shen, Z. Wu, W. Zhang, X. Xu, H. Tian, W.-H. Zhu, Y. Wu, *Sci. China Chem.* **2019**, 62, 767.

[10] X. Yang, J. Xi, Y. Sun, Y. Zhang, G. Zhou, W.-Y. Wong, *Nano Energy* **2019**, 64, 103946.

[11] B. Li, Z. Li, J. Xing, M. Zhu, Z. Zhou, *Solar RRL* **2020**, 4, 2000536.

[12] Z. Li, Y. Tong, J. Ren, Q. Sun, Y. Tian, Y. Cui, H. Wang, Y. Hao, C.-S. Lee, *Chem. Eng. J.* **2020**, 402, 125923.

[13] S. Lee, J. Lee, H. Park, J. Choi, H. W. Baac, S. Park, H. J. Park, *ACS Appl. Mater. Interfaces* **2020**, 12, 40310.

[14] J. Zhang, Q. Sun, Q. Chen, Y. Wang, Y. Zhou, B. Song, X. Jia, Y. Zhu, S. Zhang, N. Yuan, J. Ding, Y. Li, *Sol. RRL* **2020**, 4, 1900421.

[15] K. Jiang, J. Wang, F. Wu, Q. Xue, Q. Yao, J. Zhang, Y. Chen, G. Zhang, Z. Zhu, H. Yan, L. Zhu, H.-L. Yip, *Adv. Mater.* **2020**, 32, 1908011.

[16] W. Chen, Y. Wang, B. Liu, Y. Gao, Z. Wu, Y. Shi, Y. Tang, K. Yang, Y. Zhang, W. Sun, X. Feng, F. Laquai, H. Y. Woo, A. B. Djurišić, X. Guo, Z. He, *Sci. China Chem.* **2021**, 64, 41.

[17] S. Ma, X. Zhang, X. Liu, R. Ghadari, M. Cai, Y. Ding, M. Mateen, S. Dai, *J. Energy Chem.* **2021**, 54, 395.

[18] W. Yu, S. Ahmad, H. Zhang, Z. Chen, Q. Yang, X. Guo, C. Li, G. Li, *J. Energy Chem.* **2021**, 56, 127.

[19] Z. Zhou, Q. Wu, R. Cheng, H. Zhang, S. Wang, M. Chen, M. Xie, P. K. L. Chan, M. Grätzel, S.-P. Feng, *Adv. Funct. Mater.* **2021**, 31, 2011270.

[20] X. Yu, Z. Li, X. Sun, C. Zhong, Z. Zhu, Z. a. Li, A. K. Y. Jen, *Nano Energy* **2021**, 82, 105701.

[21] J. Yang, J. Huang, C. Zhang, H. Sun, B. Li, Y. Wang, K. Feng, Q. Liao, Q. Bai, L. Niu, H. Wang, X. Guo, *Adv. Funct. Mater.* **2022**, 32, 2206311.

[22] S. Huang, Z. Liu, J. Xu, D. Zhang, H. Dong, Z. Wu, L. Duan, *Chem. Eng. J.* **2022**, 430, 132986.

[23] Y. Wang, Q. Chen, J. Fu, Z. Liu, Z. Sun, S. Zhang, Y. Zhu, X. Jia, J. Zhang, N. Yuan, Y. Zhou, B. Song, Y. Li, *Chem. Eng. J.* **2022**, 433, 133265.

[24] C. Zhang, Q. Liao, J. Chen, B. Li, C. Xu, K. Wei, G. Du, Y. Wang, D. Liu,

J. Deng, Z. Luo, S. Pang, Y. Yang, J. Li, L. Yang, X. Guo, J. Zhang, *Adv. Mater.* **2023**, 35, 2209422.

[25] R. Li, J. Zhang, M. Liu, S. K. Matta, J. Tian, Z. Deng, S. P. Russo, P. Vivo, Z. Zhou, H. Zhang, *Sol. RRL* **2023**, 7, 2300031.

[26] P. Zhao, D. He, S. Li, H. Cui, Y. Yang, W. Chen, A.-S. Salah, Y. Feng, B. Zhang, *Adv. Funct. Mater.* **2024**, 34, 2308795.

[27] X. Yu, D. Gao, Z. Li, X. Sun, B. Li, Z. Zhu, Z. a. Li, *Angew. Chem. Int. Ed.* **2023**, 62, e202218752.

[28] Z. Xie, Y. Li, X. Li, Y. Fang, J. Chang, Q. Yang, X. Sun, C. Miao, G. Lu, Z. Chen, G. Li, Y. Jin, Z. Wang, X. Li, *Mater. Chem. Front.* **2024**, 8, 2764.

[29] J. Wu, L. Torresi, M. Hu, P. Reiser, J. Zhang, J. S. Rocha-Ortiz, L. Wang, Z. Xie, K. Zhang, B.-w. Park, A. Barabash, Y. Zhao, J. Luo, Y. Wang, L. Lüer, L.-L. Deng, J. A. Hauch, D. M. Guldi, M. E. Pérez-Ojeda, S. Il Seok, P. Friederich, C. J. Brabec, *Science* **2024**, 386, 1256–1264.

[30] J. Zeng, Z. Liu, D. Wang, J. Wu, P. Zhu, Y. Bao, X. Guo, G. Qu, B. Hu, X. Wang, Y. Zhang, L. Yan, A. K.-Y. Jen, B. Xu, *J. Am. Chem. Soc.* DOI: 10.1021/jacs.4c13356